Clinical Cancer Research

Induction of Telomere Dysfunction Prolongs Disease Control of Therapy-Resistant Melanoma

Gao Zhang[1], Lawrence W. Wu[1], Ilgen Mender[2], Michal Barzily-Rokni[3], Marc R. Hammond[3], Omotayo Ope[1], Chaoran Cheng[4], Themistoklis Vasilopoulos[5], Sergio Randell[1], Norah Sadek[1], Aurelie Beroard[1], Min Xiao[1], Tian Tian[4], Jiufeng Tan[1], Umar Saeed[1], Eric Sugarman[1], Clemens Krepler[1], Patricia Brafford[1], Katrin Sproesser[1], Sengottuvelan Murugan[6], Rajasekharan Somasundaram[1], Bradley Garman[7], Bradley Wubbenhorst[7], Jonathan Woo[1], Xiangfan Yin[1], Qin Liu[1], Dennie T. Frederick[8], Benchun Miao[8], Wei Xu[6], Giorgos C. Karakousis[9], Xiaowei Xu[10], Lynn M. Schuchter[6], Tara C. Mitchell[6], Lawrence N. Kwong[11], Ravi K. Amaravadi[6], Yiling Lu[12], Genevieve M. Boland[3], Zhi Wei[4], Katherine Nathanson[7], Utz Herbig[5], Gordon B. Mills[12], Keith T. Flaherty[8], Meenhard Herlyn[1], and Jerry W. Shay[2,13]

Abstract

Purpose: Telomerase promoter mutations are highly prevalent in human tumors including melanoma. A subset of patients with metastatic melanoma often fail multiple therapies, and there is an unmet and urgent need to prolong disease control for those patients.

Experimental Design: Numerous preclinical therapy-resistant models of human and mouse melanoma were used to test the efficacy of a telomerase-directed nucleoside, 6-thio-2'-deoxyguanosine (6-thio-dG). Integrated transcriptomics and proteomics approaches were used to identify genes and proteins that were significantly downregulated by 6-thio-dG.

Results: We demonstrated the superior efficacy of 6-thio-dG both *in vitro* and *in vivo* that results in telomere dysfunction, leading to apoptosis and cell death in various preclinical models of therapy-resistant melanoma cells. 6-thio-dG concomitantly induces telomere dysfunction and inhibits the expression level of AXL.

Conclusions: In summary, this study shows that indirectly targeting aberrant telomerase in melanoma cells with 6-thio-dG is a viable therapeutic approach in prolonging disease control and overcoming therapy resistance. *Clin Cancer Res; 24(19); 4771–84. ©2018 AACR.*

See related commentary by Teh and Aplin, p. 4629

Introduction

Telomerase, a ribonucleoprotein enzyme complex, is expressed in almost 90% of human tumors while most somatic tissues show no enzyme activity except in transiently proliferating stem-like cells. Therefore, telomerase remains a highly attractive target for the development of new anticancer agents. Telomerase counteracts telomere shortening by adding TTAGGG repeats at the end of chromosomes via its reverse transcriptase ribonucleoprotein complex, which is minimally composed of the catalytic protein subunit hTERT and functional RNA component hTR or hTERC.

Aberrant regulation of telomerase activity is one of the hallmarks that distinguish cancer cells from normal cells because advanced cancer cells can almost universally divide indefinitely. Owing to the maintenance of telomeres, this phenomenon is almost universally orchestrated by telomerase (1). Recent studies have revealed a high frequency of *TERT* promoter mutations, C250T and C228T in melanomas, surpassing other types of human cancers (2–10). *TERT* promoter mutations generate *de novo* consensus binding motifs for ETS transcription factors (11). Noncanonical NFκB signaling and ETS1/2 then cooperatively drive the activation of

[1]Molecular and Cellular Oncogenesis Program and Melanoma Research Center, The Wistar Institute, Philadelphia, Pennsylvania. [2]Department of Cell Biology, UT Southwestern Medical Center, Dallas, Texas. [3]Division of Surgical Oncology, Massachusetts General Hospital, Boston, Massachusetts. [4]Department of Computer Science, New Jersey Institute of Technology, Newark, New Jersey. [5]Department of Microbiology, Biochemistry, and Molecular Genetics, Rutgers Biomedical and Health Sciences, Rutgers University, Newark, New Jersey. [6]Abramson Cancer Center and Department of Medicine, Hospital of the University of Pennsylvania, University of Pennsylvania, Philadelphia, Pennsylvania. [7]Division of Translational Medicine and Human Genetics and Department of Medicine, Perelman School of Medicine at the University of Pennsylvania, Philadelphia, Pennsylvania. [8]Massachusetts General Hospital Cancer Center, Boston, Massachusetts. [9]Department of Surgery, Hospital of the University of Pennsylvania, Philadelphia, Pennsylvania. [10]Department of Pathology and Laboratory Medicine, Hospital of University of Pennsylvania, Philadelphia, Pennsylvania. [11]Department of Translational Molecular Pathology, The University of Texas MD Anderson Cancer Center, Houston, Texas. [12]Department of Systems Biology, The University of Texas MD Anderson Cancer Center, Houston, Texas. [13]Center for Excellence in Genomics Medicine Research, King Abdulaziz University, Jeddah, Saudi Arabia.

Note: Supplementary data for this article are available at Clinical Cancer Research Online (http://clincancerres.aacrjournals.org/).

Corresponding Authors: Jerry W. Shay, UT Southwestern Medical Center at Dallas, 5323 Harry Hines Boulevard, MC9039, Dallas, TX 75390-9039. Phone: 214-648-4201; Fax: 214-648-5814; E-mail: Jerry.Shay@UTSouthwestern.edu; Meenhard Herlyn, The Wistar Institute, 3601 Spruce Street, Philadelphia, PA 19104. Phone: 215-898-3950; Fax: 215-898-0980; E-mail: herlynm@wistar.org

doi: 10.1158/1078-0432.CCR-17-2773

Translational Relevance

The field has witnessed a breakthrough in the landscape of first-line and second-line therapies approved by FDA to treat unresectable or metastatic cutaneous melanoma. *BRAF*-targeted therapies and immune checkpoint blockade therapies have greatly improved patients' overall survival and progression-free survival rates. However, the long-term therapeutic outcome is often thwarted by the acquisition of therapy resistance. To date, numerous mechanisms underlying therapy resistance have been documented, which present a great challenge in identifying a universal therapeutic approach that has the potential to overcome multidrug resistance. This study presents preclinical evidence demonstrating the efficacy and potency of 6-thio-dG in overcoming therapy resistance via the induction of telomere dysfunction.

the C250T-mutant *TERT* promoter and increase *TERT* levels and enzyme activity (12). The *de novo* ETS motif is critical for mutant *TERT* promoter activity and facilitates heterotetramer binding of GABP to the mutant *TERT* promoter (13).

BRAF-mutated cutaneous melanomas inevitably acquire resistance to inhibitors targeting the MAPK pathway (MAPKi) that are active in *BRAF*-mutated tumors. Molecular mechanisms underlying both intrinsic and acquired resistance to mutant *BRAF*-targeted therapies are highly complex and variable (14–16). This warrants the identification of actionable therapies that are personalized and tailored to each therapy-resistant tumor's genetic composition and proteomic profiles.

Immune checkpoint blockade therapies have also emerged as first-line therapies for treating patients with unresectable or metastatic melanomas. For treatment-naïve patients enrolled in a randomized phase III study, the objective response rate was 19%, 43.7%, and 57.6%, respectively, for ipilimumab, nivolumab, and nivolumab plus ipilimumab (17). However, depending on the therapy arm, almost half of the patients progressed despite the initial success of immunotherapy. This suggests that combinational or additional drugs administered in sequence might potentially prolong clinical responses.

Taken together, there remains a large unmet and urgent need to identify novel therapies for treating patients with metastatic melanoma who have had disease progression after first-line therapies. Our previous study demonstrated that the induction of telomere dysfunction by telomerase-directed 6-thio-2'-deoxyguanosine (6-thio-dG) therapy significantly impairs viability and proliferation of telomerase-positive lung and colon cancer cells but not telomerase-negative normal cells (18). We reason that targeting telomerase might provide a novel therapeutic approach for treating patients with unresectable or metastatic melanoma whose disease has progressed. In this study, we show the broad efficacy of the telomerase-directed 6-thio-dG in multiple preclinical models of therapy-resistant human and mouse melanomas.

Materials and Methods

Ethics statement

All clinical data and patient samples were collected following approval by the Massachusetts General Hospital Institutional Review Board (IRB) and the Hospital of the University of Pennsylvania IRB. In all cases informed consent was obtained from patients. All animal studies were conducted in accordance with the Guide for the Care and Use of Laboratory Animals of the NIH. Mice were maintained according to the guidelines issued by Institutional Animal Care and Use Committee (IACUC) at The Wistar Institute (Philadelphia, PA). Study designs were approved by IACUC at The Wistar Institute (Philadelphia, PA).

Cell lines and short-term primary cultures

All normal skin epidermal melanocytes, keratinocytes, and human metastatic melanoma cell lines that were established at The Wistar Institute (Philadelphia, PA) and methods that were used for the routine authentication and mycoplasma test of cell lines have been documented in https://www.wistar.org/our-scientists/meenhard-herlyn. UACC-62 and UACC-903 cells were kind gifts from Dr. Marianne B. Powell (Stanford University, Stanford, CA). A375 cells were purchased from ATCC. LOX-IMVI cells were kindly provided by Dr. Lin Zhang (University of Pennsylvania, Philadelphia, PA). 499 and JB2 cells were kind gifts from Dr. Andy Minn (University of Pennsylvania, Philadelphia, PA). All resistant cell lines that acquired drug resistance to BRAF inhibitor or the combination of BRAF inhibitor plus MEK inhibitor were described previously (19, 20). All cell lines were maintained in RPMI1640 media (Mediatech, Inc.) supplemented with 10% FBS (Tissue Culture Biologicals) and cultured in a 37°C humidified incubator supplied with 5% CO_2.

Chemicals

The BRAF inhibitor PLX4720 was provided by Plexxikon Inc. The BRAF inhibitor dabrafenib, the apoptosis inducer staurosporine, and the pan-caspase inhibitor Z-VAD-FMK were purchased from LC Laboratories. The MEK inhibitor PD0325901 was purchased from Selleckchem. 6-thio-dG used for *in vitro* studies was purchased from Metkinen Chemistry Oy. 6-thio-dG used for *in vivo* studies was purchased from R I Chemical Inc. The telomerase inhibitor, BIBR 1532 was purchased from Cayman Chemical. The lipid modified 13-mer thio-phosphoramidate oligonucleotide is a telomerase template antagonist GRN163L (Imetelstat) as described previously (21).

Melanoma xenotransplantation and *in vivo* studies

A total of 1×10^5 melanoma cells were harvested from cell culture and resuspended in culture medium and Matrigel at a 1:1 ratio. Cells were subcutaneously injected into mice, which were treated with indicated inhibitors once daily via intraperitoneal (IP) administration (6-thio-dG) or oral gavage (dabrafenib) when the tumor volume reached the range of 50–100 mm^3. Mice were sacrificed at the end time point and solid tumors were collected. All animal experiments were performed in accordance with Wistar IACUC protocol 112330 in NOD.Dg-Prkdc scidIL2rg tm 1 Wjl/SzJ mice.

RNA purification, library preparation, and sequencing

RNA purification was done using the AllPrep DNA/RNA Mini Kit (Qiagen) for 31 tumor biopsy specimens. The first batch of 17 RNA samples were ribo-zero treated and then subject to library preparation using Epicentre ScriptSeq Complete Gold kit. Quality check was done on the Bioanalyzer using the High Sensitivity DNA kit and quantification was carried out using KAPA Quantification kit. Samples were sequenced on Illumina NextSeq500 with the 2×75 bp high output in the Genomics Core Facility at The Wistar Institute (Philadelphia, PA). The second batch of 14 RNA samples purified from tumor biopsy specimens along and

the third batch of 12 RNA samples purified from A375 and LOX-IMVI BR cells were sequenced at Broad Institute to achieve the high coverage of 50M pairs. Briefly, the Tru-Seq Non-Strand Specific RNA Sequencing, which includes plating, poly-A selection, and nonstrand-specific cDNA synthesis, library preparation, sequencing, and sample identification QC check (when Sample Qualification of a matching DNA sample is chosen). RNA-seq data of A375 and LOX-IMVI BR cells were deposited into Gene Expression Omnibus (accession number GSE99552).

FACS analysis of apoptosis and cell death

Adherent cells were harvested with 0.05% Trypsin-EDTA, pooled with floating cells and then washed once with 1× DPBS. Cells were then pelleted and stained with PSVue 643 at 0.5 μmol/L and propidium iodide at 50 μg/mL diluted in TES buffer for 5 minutes in the dark. Cells were then immediately subjected to FACS analysis using a BD LSR II flow cytometer and at least 5,000 cells per sample were acquired.

Assessment of cell clonogenicity

Cells were seeded into 12-well tissue culture plates at a density of 500 cells/well as biological triplicates in drug-free medium. Medium was refreshed every 3 or 4 days for 14 days. Colonies were then stained overnight with methanol containing 0.05% crystal violet. After extensive washing with distilled H_2O, cells were air-dried and subjected to image acquisition using a Nikon D200 DLSR camera.

Gene expression microarray, RNA sequencing, and reverse-phase protein array data

The source and analysis of gene expression microarray data, RNA-sequencing (RNA-seq) data, and reverse-phase protein array (RPPA) of melanoma cell lines or paired pre- and posttreatment tumor biopsies derived from patients with metastatic melanoma were previously described (19, 20).

Droplet digital TRAP (ddTRAP) assay

The quantitation of telomerase enzyme activity was performed as described previously (22).

Hematoxylin and eosin and IHC staining

The hematoxylin and eosin (H&E) and IHC staining of tumor and liver specimens was performed as described previously (19, 20). Ki-67, AXL, and phospho-S6 antibodies were purchased from Cell Signaling Technology (catalog nos. are 9027, 8661, and 4858).

Knockdown of *TERT* by RNA interference

pMKO.1-GFP (https://www.addgene.org/10676/) and pMKO.1-shTERT (https://www.addgene.org/10688/) plasmids obtained from Addgene. For the retroviral production, the platinum A cell line (Cell Biolabs) was transfected with pMKO.1-GFP and pMKO.1-shTERT plasmids using the Calcium Phosphate method. Twenty-four hours after transfection, the fresh medium was added. Starting from day 2 after the initial transfection, viral supernatants were collected for two consecutive days. Viral supernatants were centrifuged at 1,200 rpm for 5 minutes and filtered using 0.45-μm filters. A375 cells were infected with viral supernatants supplemented with Polybrene at 8 μg/mL. Stably infected cells were established by either FACS sorting of GFP-positive cells or puromycin selection.

Statistical analysis

Unless otherwise indicated, data in the figures were presented as mean ± SEM for three biological or technical replicates. Significant differences between experimental conditions were determined using the two-tailed unpaired *t* test. For survival data, Kaplan–Meier survival curves were generated and their differences were examined with log-rank test. For tumor growth data, mixed effect models were used to determine the differences between treatment groups in tumor volume change at the end of experiment. A two-sided *P* value of less than 0.05 was considered statistically significant (*, $P < 0.05$; **, $P < 0.005$; ***, $P < 0.0005$).

Results

6-thio-dG only impairs cell viability of telomerase-positive cancer cells

We previously demonstrated that 6-thio-dG inhibited cell viability of the colon cancer cell line, HCT116 and the non–small cell lung cancer cell line, A549 (18). Next, we set out to test the efficacy of 6-thio-dG in the genetic subtype of *BRAF*-mutated melanoma. We treated the first cohort of 12 human metastatic melanoma cell lines harboring the $BRAF^{V600E}$ mutation with 6-thio-dG for 9-12 days. As controls for 6-thio-dG, we also tested the analogue of 6-thio-dG, 6-thioguanine and a well-known telomerase inhibitor, BIBR 1532 (23). Interestingly, we observed a marked antiproliferative effect of 6-thio-dG in *BRAF*-mutated melanoma cell lines, which is superior compared with that of BIBR 1532 (Fig. 1A). In contrast, we showed that 6-thio-dG did not impair the cell viability of normal human skin cells, including keratinocytes (FK170), melanocytes (FOMG005), and fibroblasts (GM21), whereas the apoptosis inducer Staurosporine significantly induced apoptosis and cell death by day 4 (Fig. 1B; ref. 24). Our findings are consistent with our previous study showing that human normal fibroblasts and colonic epithelial cells were not as sensitive to 6-thio-dG as telomerase–positive cancer cells (18). Taken together, our results suggest telomerase-positive *BRAF*-mutated melanoma cells are sensitive to 6-thio-dG.

6-thio-dG impairs cell viability and tumor growth of *BRAF*-mutant melanoma cells

The investigation of *BRAF*-mutated melanoma cell lines allowed us to compare the efficacy of 6-thio-dG with that of a BRAF inhibitor, PLX4720. We treated the second cohort of 16 *BRAF*-mutant melanoma cell lines with 6-thio-dG and PLX4270 for 9–12 days, respectively. There were three melanoma cell lines that overlapped in both cohorts, including A375, SK-MEL-28, and WM793 (Figs. 1A and 2A–D). We demonstrated that 6-thio-dG also substantially inhibited cell viability of *BRAF*-mutated melanoma cell lines in the second cohort and the efficacy of 6-thio-dG was comparable with and in some cases even superior to that of PLX4720 (Fig. 2A–D; Supplementary Table S1).

TERT promoter mutations are known for 9 and 16 *BRAF*-mutated human melanoma cell lines included in the first (Fig. 1A) and second cohort (Fig. 2A–D), respectively. WM278, WM35, and WM793 melanoma cell lines harbor wild-type *TERT* promoter and they responded well to 6-thio-dG (Fig. 2A–D). Therefore, we reasoned that the status of *TERT* promoter mutation is unlikely to be associated with responses of *BRAF*-mutated melanoma cell lines to 6-thio-dG.

Treatment of 12 *BRAF*-mutated melanoma cell lines with 6-thio-dG over a shorter period of 5 days significantly induced apoptosis and cell death in 9 of them (Supplementary Fig. S1A). A375 was the one with the highest sensitivity to 6-thio-dG (Supplementary Fig. S1A). Using A375 as a representative cell

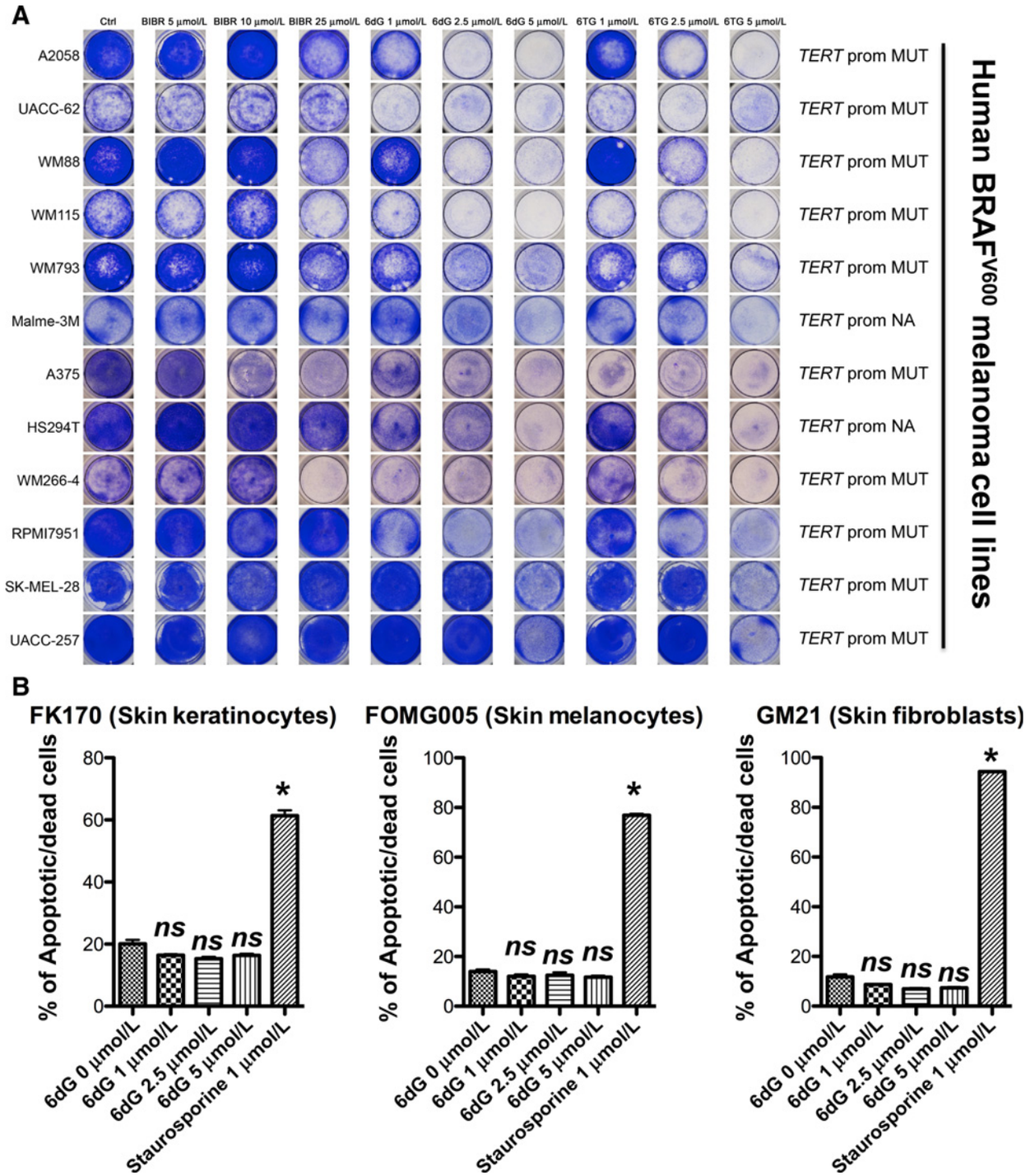

Figure 1.

6-thio-dG impairs cell viability of 12 *BRAF*-mutant melanoma cell lines but not human normal skin cells. **A,** Long-term cell growth assay of 12 *BRAF*-mutant melanoma cell lines that were treated with the control (Ctrl), BIBR 1532 (BIBR), 6-thio-dG (6dG), or 6-thioguanine (6TG) at indicated doses for 9 to 12 days. Cells were then fixed and stained with crystal violet. Representative image of two biological replicates were shown for each experimental condition. "WT" indicates wild-type *TERT* promoter; "MUT" indicates mutant *TERT* promoter; "NA" indicates that TERT promoter mutation is unknown. **B,** Percentage of apoptotic and dead cells in normal skin melanocytes (middle), keratinocytes (left), and fibroblasts (right) that were treated with 6-thio-dG at indicated doses and staurosporine at 1 μmol/L, respectively, for 96 hours. Cells were then harvested and costained with PSVue643 and propidium iodide (PI). Representative samples of two independent experiments.

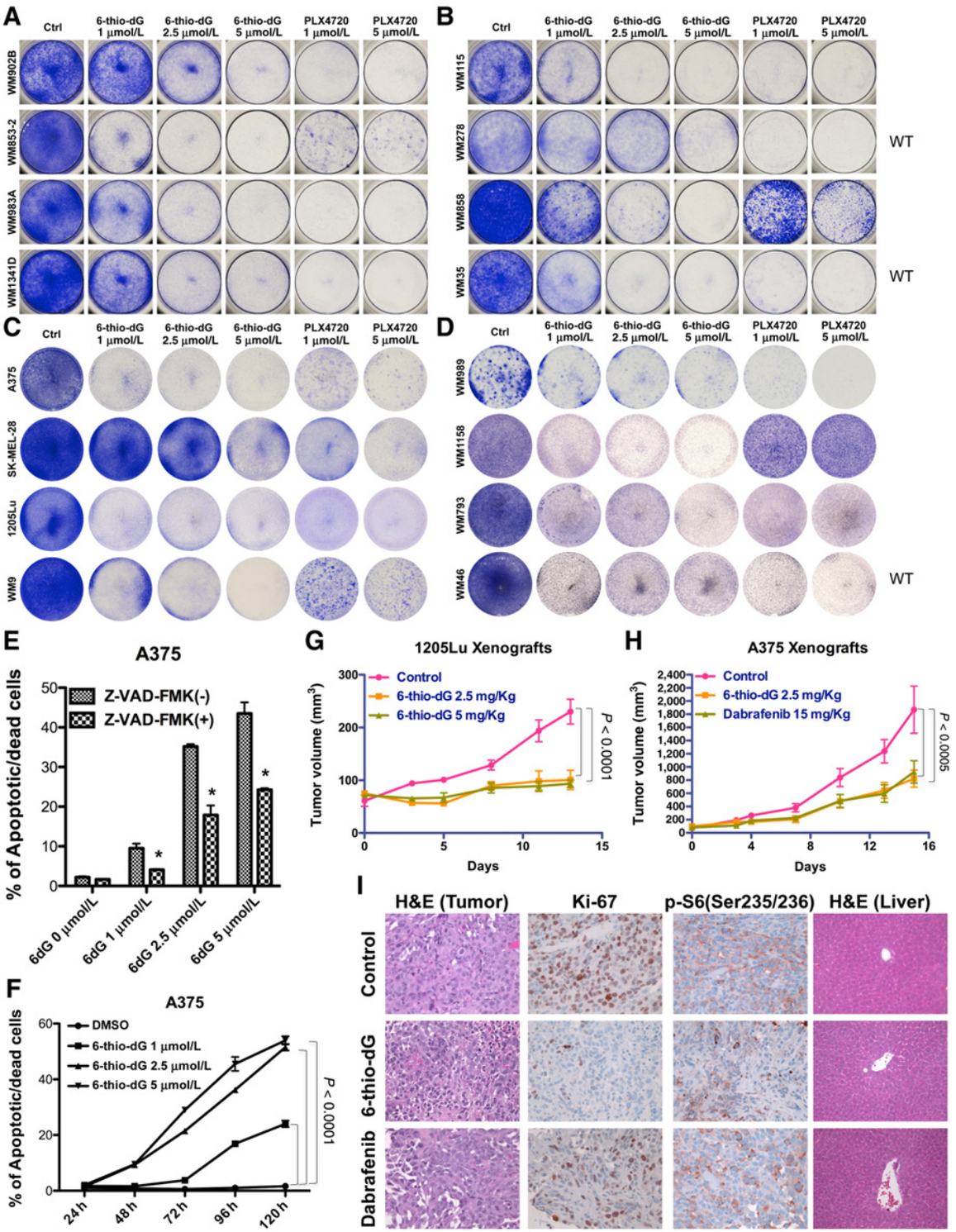

Figure 2.

6-thio-dG impairs cell viability and inhibits tumor growth of *BRAF*-mutant melanoma cells. **A–D,** Long-term cell growth assay of 16 *BRAF*-mutant melanoma cell lines that were treated with 6-thio-dG or PLX4720 at indicated doses for 12 days. Cells were then fixed and stained with crystal violet. Representative image of two biological replicates were shown for each experimental condition. **E** and **F,** Percentage of apoptotic and dead cells indicated as PSVue 643^{+} cells in A375 cells treated with 6-thio-dG at titrated doses for 72 hours in the presence or absence of staurosporine at 1 μmol/L (**E**) or with 6-thio-dG at titrated doses for 120 hours (**F**). Cells were then harvested and costained with PSVue643 and propidium iodide (PI). **G** and **H,** Tumor volumes of 1205Lu and A375 xenografts that were treated with the vehicle control, 6-thio-dG, and dabrafenib at indicated doses. **I,** H&E staining of A375 tumors from **H** and livers from mice bearing A375 tumors. The IHC analysis of Ki-67 and phospho-S6 was also performed in A375 tumors.

line, we showed that the addition of a pan-caspase inhibitor (Z-VAD-FMK) significantly decreased the percentage of apoptotic and dead cells treated with 6-thio-dG for 72 hours (Fig. 2E). In a time-course experiment, we further demonstrated that the induction of apoptosis and cell death in A375 cells treated with 6-thio-dG at 2.5 and 5 μmol/L could occur as early as 48 hours posttreatment (Fig. 2F).

The induction of apoptosis and cell death prompted us to also investigate cells that had survived 6-thio-dG. The senescence-associated β-gal (SA-β-gal) staining of 4 *BRAF*-mutated melanoma cell lines suggested that long-term treatment with 6-thio-dG triggered induction of cellular senescence in cells that survived the initial killing by 6-thio-dG (Supplementary Fig. S1B).

Finally, we established xenografts of 1205Lu and A375 melanoma cell lines and showed that 6-thio-dG significantly impaired the tumor growth of both xenograft models following intraperitoneal administration (Fig. 2G and H). Of note, the efficacy of 6-thio-dG was comparable with that of dabrafenib that is a BRAF inhibitor approved by FDA to treat patients with *BRAF*-mutated melanoma as shown in A375 xenografts (Fig. 2H). Neither 6-thio-dG nor dabrafenib significantly decreased mouse weight in both xenograft models (Supplementary Fig. S1C and S1D). Both 6-thio-dG and dabrafenib substantially inhibited the protein expression of Ki-67 and phospho-S6 in A375 xenografts (Fig. 2I). The H&E staining of liver tissues from mice bearing A375 xenografts treated with 6-thio-dG or dabrafenib did not show any signs of toxicities (Fig. 2I). Taken together, our data highlight the superior antitumor activity and specificity of 6-thio-dG as seen both *in vitro* and *in vivo*.

Transcriptional signaling pathways and proteins downregulated by 6-thio-dG

The short-term treatment of A375 melanoma cells with 6-thio-dG but not BIBR 1532 (a telomerase inhibitor) significantly induced apoptosis and cell death (Fig. 3A). To gain mechanistic insights into the antitumor activity of 6-thio-dG, we treated A375 cells with the control, BIBR 1532, and 6-thio-dG for 48 hours, respectively. We profiled the transcriptome with RNA sequencing (RNA-seq) and the functional proteome with reverse-phase protein array (RPPA).

The differential gene expression analysis identified genes that were significantly up- and downregulated in A375 cells treated with 6-thio-dG and BIBR 1532, respectively (Supplementary Table S2 and S3). Among them were *CD274* (*PD-L1*) and *c-Myc* that showed the highest degrees of inhibition, which were not inhibited in A375 cells treated with BIBR 1532 (Fig. 3B and C).

To further unravel the signaling pathways altered in A375 cells treated with 6-thio-dG or BIBR 1532, we carried out the hypergeometric differential analysis by focusing on those significantly downregulated genes. This analysis demonstrated that BioCarta gene sets related to "cell cycle" and "telomere biology" were among the top 10 ranked (Fig. 3D and E). Next, we utilized a complementary approach, single-sample gene set enrichment analysis (ssGSEA) and demonstrated that a broad collection of all of 11 telomere-related gene sets were indeed suppressed to a larger degree in A375 cells treated with 6-thio-dG compared with those treated with BIBR 1532 (Fig. 3F). Furthermore, we calculated ssGSEA scores of these 11 telomere-related gene sets in 18 CCLE melanoma cell lines and investigated correlations between ssGSEA scores and sensitivities of these cell lines to 6-thio-dG (Supplementary Table S4). We identified that three telomere-related gene sets were positively and significantly correlated with drug sensitivities, including "Telomere Maintenance," "TERT Targets," and "Telomerase Activity" (Fig. 3G–I). Not surprisingly, when *TERT* was depleted in A375 cells leading to a decrease in telomerase activity (Fig. 3J and K), the drug sensitivity to 6-thio-dG was significantly decreased (Fig. 3L). Taken together, our data suggested that the action mode of 6-thio-dG is dependent on telomerase activity and telomere maintenance.

Subsequently, we analyzed RPPA data and identified 30 proteins that were significantly downregulated in A375 cells treated with 6-thio-dG. This analysis revealed that three major signaling pathways were suppressed in A375 cells treated with 6-thio-dG. They were (i) cell cycle: phospho-RB$^{Ser807/811}$, cyclin B1, CDK1, FOXM1, PLK1 and AURKB; (ii) DNA damage response: 53BP1, ATM, ATR, CHK1 and CHK2; and (iii) receptor tyrosine kinase signaling: VEGFR, PDGFRb, IGF-IRb, IGFBP2, phospho-STAT3^{Y705} and phospho-HER3^{Y1289} (Fig. 3M). We also validated most of the downregulated proteins by Western blotting and showed that these proteins were indeed decreased in A375 cells treated with 6-thio-dG but not BIBR 1532 or another telomerase inhibitor, GRN163L (imetelstat; Fig. 3N and O; ref. 21). Conversely, the analysis also identified 30 proteins that were significantly upregulated in A375 cells treated with 6-thio-dG. The major signaling pathways that were upregulated were: (i) cell cycle: p53 and p21; (ii) apoptosis: Bax, caspase-3, and cleaved caspase-7; (iii) AKT signaling: phospho-AKT^{T308} and phospho-AKT^{S473} (Supplementary Table S5).

Because both analyses of RNA-seq and RPPA data suggested that the cell-cycle pathway is altered, we exploited A375^{Fucci2} cells expressing the "fluorescent, ubiquitination-based, cell-cycle indicators Fucci, version 2" reporter construct to visualize cell-cycle progression when cells were treated with 6-thio-dG. Time-lapse imaging showed that A375^{Fucci2} cells treated with 6-thio-dG over 42 hours were arrested at the G_2–M checkpoint followed by cell death (Supplementary Movie S1 and S2).

6-thio-dG significantly impairs cell viability, proliferation, and tumor growth of therapy-resistant melanoma cells

BRAF inhibitors (BRAFi) or the combination of BRAF inhibitors plus MEK inhibitors (MEKi) exhibit superior antitumor activity in *BRAF*-mutated melanoma cells but the development of acquired resistance inevitably occurs. This presents a great challenge in overcoming therapy resistance. To address this, we established a large panel of human melanoma cell lines that acquired resistance to BRAFi, MEKi, or the combination of BRAFi plus MEKi (19, 20). First, we asked whether therapy-resistant melanoma cells were sensitive to 6-thio-dG. Treatment of ten melanoma cell lines that had acquired resistance to PLX4720 and one melanoma cell line, WM1366 MEKi-resistant (MR) that acquired resistance to a MEK inhibitor (MEK162) with 6-thio-dG for 12 days showed a general sensitivity to 6-thio-dG and reduced viability (Fig. 4A; Supplementary Fig. S2A; Supplementary Table S6; refs. 19, 20). Next, we demonstrated that the short-term treatment of LOX-IMVR BR cells with 6-thio-dG significantly and rapidly induced apoptosis as well as cell death in the cells (Fig. 4B). Treatment of LOX-IMVI BR cells with 6-thio-dG for 120 hours led to progressive telomere shortening in residual cells (Fig. 4C). Compared with the control, 6-thio-dG also induced DNA damage (Fig. 4D–F) and led to an increase in telomere dysfunction-induced foci (TIF) that can be observed as colocalization of a specific γH2AX antibody with an *in situ* telomere-specific hybridization probe (Fig. 4D, E, and G).

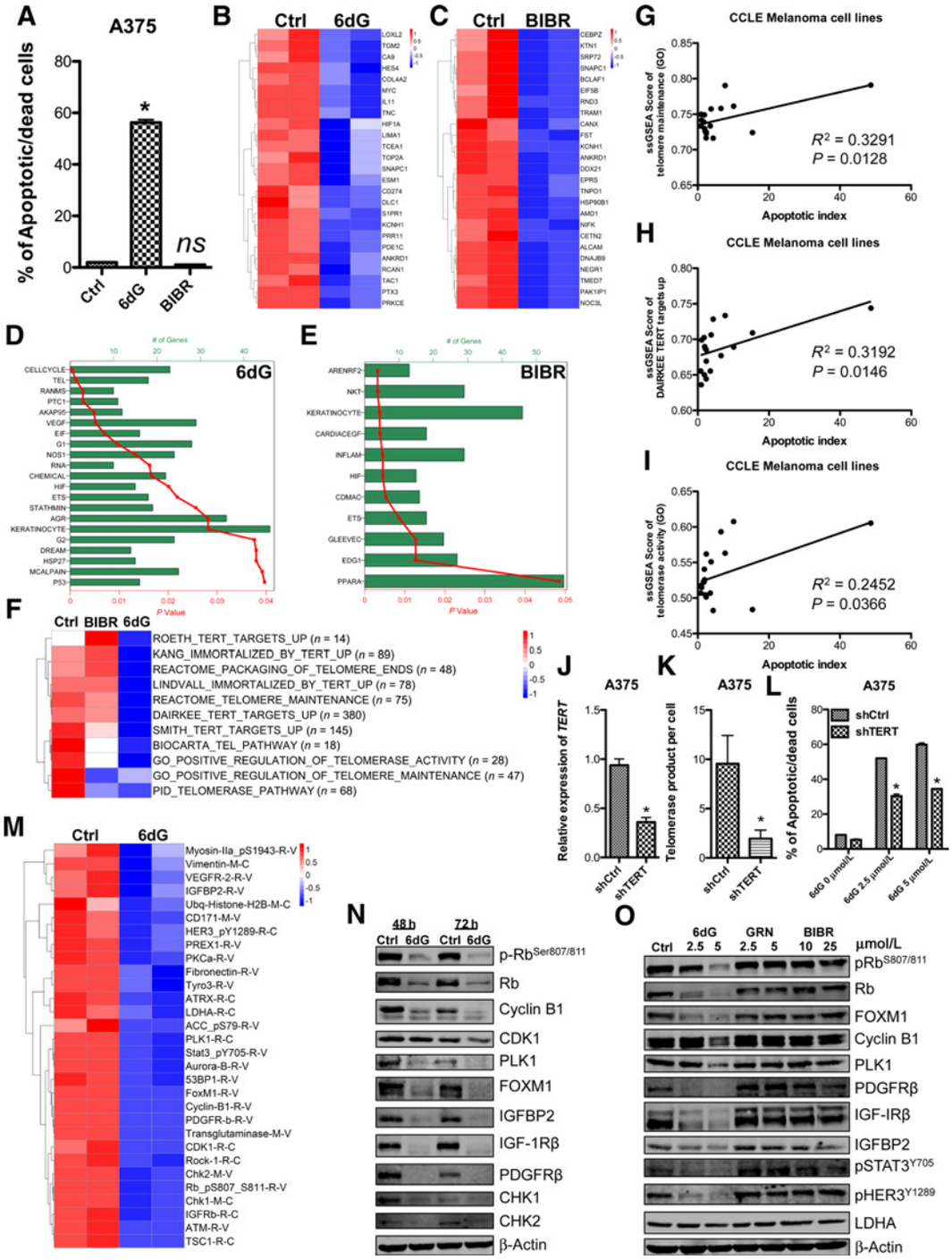

Figure 3.

The functional proteomic analysis of A375 cells treated with 6-thio-dG reveals a protein expression signature of 6-thio-dG. **A,** Percentage of apoptotic and dead cells indicated as PSVue 643^{+} cells in A375 cells treated with 6-thio-dG (6dG) and BIBR 1532 (BIBR), respectively, for 72 hours. The heatmaps of RNA-seq data depicting genes that were most significantly downregulated in A375 cells treated with 6-thio-dG (6dG; **B**) or BIBR 1532 (BIBR; **C**) for 72 hours. Two biological replicates were shown for each experimental condition. The plot of Biocarta gene sets that were most significantly altered in A375 cells treated with 6-thio-dG (6dG; **D**) or BIBR 1532 (BIBR; **E**) as determined by the hypergeometric differential analysis. **F,** The ssGSEA plot of 11 MSigDB gene sets related to telomere and telomerase that were significantly altered in A375 cells treated with BIBR 1532 (BIBR) or 6-thio-dG (6dG). **G–I,** The plot showing the correlation between the ssGSEA score of "Telomere Maintenance" (**G**), "TERT Targets Up" (**H**), and "Telomerase Activity" (**I**) and apoptotic index of 18 CCLE melanoma cell lines. **J,** The relative expression level of *TERT* in A375 control cells (shCtrl) and A375 cells expressing the shTERT construct. **K,** The telomerase product per cell in A375 cells from **J**. **L,** Percentage of apoptotic and dead cells indicated as PSVue 643^{+} cells in A375 cells from **J** treated with 6-thio-dG (6dG) at indicated doses for 72 hours. **M,** The heatmap of RPPA data depicting 30 proteins that were most significantly downregulated in A375 cells treated with 6-thio-dG (6dG) for 72 hours. Two biological replicates were shown for each experimental condition. **N** and **O,** Western blotting of proteins that were downregulated in A375 cells treated with 6-thio-dG (6dG) for 48 and 72 hours (**M**) or 6-thio-dG (6dG), Imetelstat, also known as GRN163L (GRN), or BIBR 1532 (BIBR) for 48 hours (**O**) as identified by RPPA.

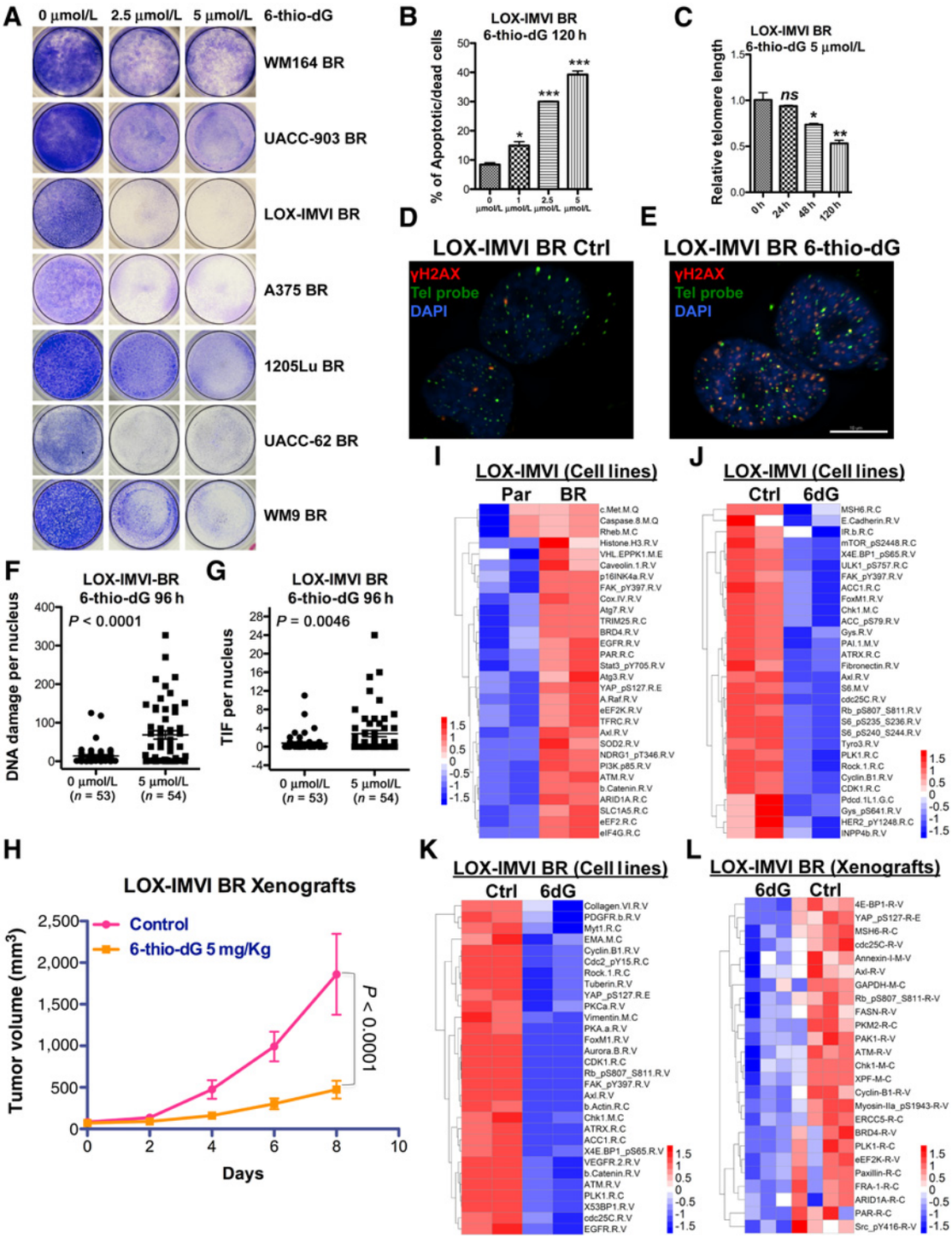

Figure 4.

6-thio-dG overcomes acquired resistance to MAPKi. **A,** Long-term cell growth assay of 7 melanoma BR cell lines treated with 6-thio-dG at indicated doses for 12 days. Cells were then fixed and stained with crystal violet. A representative image of two biological replicates is shown for each experimental condition. **B,** Percentage of apoptotic and dead cells indicated as PSVue 643^{+} cells for LOX-IMVI BR cells that were treated with the control or 6-thio-dG at indicated doses for 120 hours. The average of two biological replicates was plotted, and data are representative of two independent experiments. **C,** The telomere length was measured in LOX-IMVI BR cells treated with 6-thio-dG at 5 μmol/L collected at different time points as shown in **B**. **D** and **E,** Costaining of γH2AX antibody (double-strand DNA damage marker) with an *in situ* telomere-specific hybridization probe [FITC-conjugated telomere sequence $(TTAGGG)_3$ peptide nucleic acid] in LOX-IMVI BR cells treated with the control (**D**) and 6-thio-dG (**E**). **F** and **G,** Quantification of DNA damage foci (**F**) and TIF (**G**) for samples shown in **D** and **E**. **H,** Tumor volumes of xenografts LOX-IMVI BR cells treated with the vehicle control or 6-thio-dG administered intraperitoneally daily. **I,** The heatmap of 30 proteins that were significantly upregulated in LOX-IMVI BR cells compared with parental cells. **J–L,** The heatmap of 30 proteins that were significantly downregulated in LOX-IMVI cells (**J**), LOX-IMVI BR cells (**K**), and LOX-IMVI BR xenografts (**L**) treated with 6-thio-dG compared with the control samples.

Having demonstrated the efficacy of 6-thio-dG in treating targeted therapy-resistant melanoma cell lines *in vitro*, we further showed that 6-thio-dG adminstered intraperitoneally daily significantly impaired the *in vivo* growth of four xenografts derived from LOX-IMVI BR (Fig. 4H), WM9 BR, UACC-903 BR, and A2058 CR cells that are resistant to the BRAFi or the combination of BRAFi plus MEKi (Supplementary Fig. S2B–S2D).

We then carried out RNA-seq to profile the transcriptome of LOX-IMVI BR cells treated with 6-thio-dG. Using the ssGSEA approach, we demonstrated that all of 11 telomere-related gene sets were suppressed to a larger degree in LOX-IMVI BR cells treated with 6-thio-dG compared with those treated with BIBR 1532, which is in line with data based on A375 cells treated with 6-thio-dG (Supplementary Fig. S2E).

Next, we conducted RPPA experiments to analyze LOX-IMVI parental and BR melanoma cells that were grown *in vitro* or *in vivo* and treated with 6-thio-dG (Fig. 4I–L; Supplementary Tables S7–S10). The analysis of RPPA data of LOX-IMVI therapy-naïve and resistant cells revealed a number of proteins that were significantly upregulated in LOX-IMVI BR cells, including phospho-FAK^{Y397}, BRD4, EGFR, phospho-STAT3^{Y705}, phospho-YAP^{S127}, A-RAF, AXL, PI3K p85, and β-Catenin, many of which were reported to cause resistance to targeted therapy (Fig. 4I; Supplementary Table S7). Similar to A375 cells treated with 6-thio-dG, the analysis of RPPA data of LOX-IMVI BR cells showed that, three major signaling pathways were altered in LOX-IMVI BR cells treated with 6-thio-dG. They were (i) cell cycle: phospho-RB$^{Ser807/811}$, cyclin B1, CDK1, FOXM1, PLK1, AURKB, Cdc25C, and p-Cdc2^{Y15}; (ii) DNA damage response: 53BP1, ATM, and CHK1; (iii) receptor tyrosine kinase signaling: VEGFR and PDGFRβ (Fig. 4K; Supplementary Table S9). In addition, other functionally important proteins were also downregulated, including AXL, phospho-YAP^{S127}, phospho-FAK^{Y397}, phospho-4E-BP1^{S65}, and β-catenin (Fig. 4K; Supplementary Table S9). It is of particular interest to note that two proteins, AXL and phospho-YAP^{Ser127}, were significantly upregulated in LOX-IMVI BR cells compared with the control cells and downregulated in LOX-IMVI BR cells or xenografts treated with 6-thio-dG (Fig. 4K and L; Supplementary Table S9 and S10; ref. 25). RPPA profiling of another panel of four MAPKi-resistant cell lines treated with 6-thio-dG revealed changes at the protein level that were similar to those observed in LOX-IMVI BR cells, including the significant downregulation of AXL (Supplementary Fig. S2F–S2I). The Western blotting and IHC analyses further confirmed the downregulation of AXL in LOX-IMVI BR cells (Supplementary Fig. S2J) and A375 xenografts (Supplementary Fig. S2K) treated with 6-thio-dG, respectively.

Starting with A375^{Fucci2} cells, we also established A375^{Fucci2}-BR and A375^{Fucci2}-CR cells that acquired resistance to the BRAFi and the combination of the BRAFi plus the MEKi, respectively. Not surprisingly, we found that treatment of A375^{Fucci2}-BR or A375^{Fucci2}-CR cells with 6-thio-dG also led to the cell-cycle arrest and the induction of cell death as demonstrated by the time-lapse imaging (Supplementary Movie S3–S6).

Association of gene signatures of telomere and telomerase with therapy resistance

Next, we extended this study from the investigation of established human melanoma cell lines to the analysis of RNA-seq data of paired pre-, on-, and posttreatment tumor biopsies derived from patients with metastatic melanoma who progressed on targeted therapies or immunotherapies. First, we analyzed RNA-seq data derived from patients with advanced *BRAF*-mutated melanoma whose tumors progressed on molecularly targeted therapies. The ssGSEA approach identified "packaging of telomere ends" and "telomere maintenance" as being highly enriched in a subset of posttreatment tumor biopsies procured at the time of disease progression on BRAFi or the combination therapy of BRAFi plus MEKi compared with paired pretreatment tumor biopsies (Fig. 5A; Supplementary Fig. S3A–S3C).

Next, to investigate whether the activation of telomere signaling axis also mediates resistance to immune checkpoint blockade therapies, we first analyzed RNA-seq data of 14 posttreatment tumor biopsy specimens derived from patients with metastatic melanoma treated with ipilimumab at Memorial Sloan Kettering Cancer Center (New York, NY; refs. 26, 27). Specifically, we compared tumor biopsy specimens derived from patients experiencing "no clinical benefit" to those derived from patients experiencing "long-term clinical benefit." We identified genes that were differentially expressed between "no clinical benefit" and "long-term clinical benefit" subgroups and then carried out GSEA to identify pathways that were associated with the phenotype of "no clinical benefit." Interestingly, a highly ranked gene set is the "BioCarta TEL pathway" that is comprised of genes related to telomeres, telomerase, cellular aging, and immortality (Fig. 5B).

Finally, we carried out RNA-seq of paired pre-, on-, and/or posttreatment tumor biopsies derived from 16 patients with metastatic melanoma who were treated with various immune checkpoint blockade therapies at Massachusetts General Hospital (Boston, MA). The best response for most of those patients was progressive disease. The ssGSEA identified "packaging of telomere ends" and "telomere maintenance" being highly enriched in 8 out 16 patients' on- or posttreatment tumor biopsies (Supplementary Table S7). For example, "packaging of telomere ends" was highly enriched in 5 out of 8 early on-αCTLA-4 tumor biopsies (Fig. 5C), 5 out of 10 early on-αPD1 tumor biopsies (Fig. 5D), 1 out of 3 early on- αPD-L1 tumor biopsies (Fig. 5E), 4 out of 7 post-αCTLA-4 tumor biopsies (Fig. 5F), and 2 out of 2 post-αPD1 tumor biopsies (Fig. 5G).

In summary, this computational analysis reveals the reactivation of telomere signaling axis in on- and/or posttreatment tumor specimens derived from patients treated with immune checkpoint blockade therapy. This suggests that a viable approach of targeting the aberrant telomere signaling in combination with αCTLA-4, αPD-1, and/or αPD-L1 therapies could be considered.

6-thio-dG significantly impairs cell viability, proliferation, and tumor growth of melanoma cells that are resistant to immune checkpoint inhibitors

Having demonstrated the efficacy of 6-thio-dG in inhibiting *in vivo* growth of MAPKi-resistant tumors and established the reactivation of telomere signaling axis in on- or posttreatment tumor biopsies derived from patients treated with immune checkpoint blockade therapies, we then examined the ability of 6-thio-dG to inhibit both *in vitro* and *in vivo* growth of melanoma cells derived from tumor specimens that are resistant to immune checkpoint inhibitors. First, we established two short-term primary cultures, T708-13-456-3-3 and T708-13-456-5-3, from two distinct *BRAF*^{V600E}-positive melanoma breast metastases that were surgically removed from a patient who progressed on sequential therapies including radiotherapy, ipilimumab, temozolomide, and pembrolizumab. Second, we established a short-term primary culture, 15-1761-1-2, from a left axillary lymph node

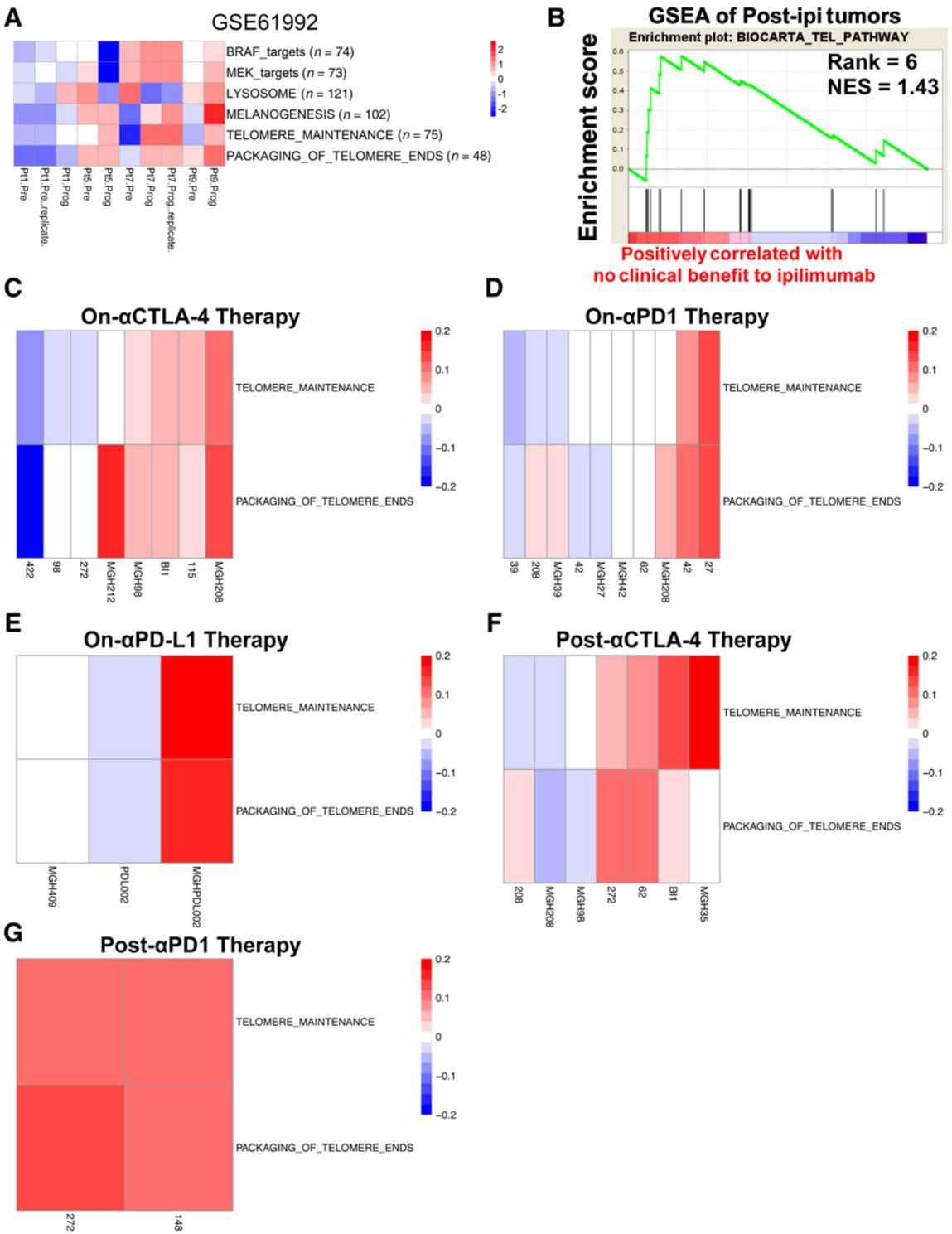

Figure 5.

The expression of telomere transcriptional gene signatures in on- or posttreatment tumor biopsies derived from patients treated with first-line therapies. **A,** The heatmap of two telomere transcriptional gene signatures, two melanoma-specific gene sets, and two MAPK pathway–related gene sets in GSE61992 in which transcriptomes of patients' paired pre- and posttreatment tumor biopsies were profiled. **B,** The GSEA plot of the "Biocarta Tel Pathway" gene set that was enriched in posttreatment tumor biopsies derived from patients from Memorial Sloan Kettering Cancer Center who did not experience long-term benefit from ipilimumab. **C–G,** Heatmaps of the ssGSEA score of on- or posttreatment tumor biopsies subtracted from that of the paired pretreatment tumor biopsies derived from patients treated with immune checkpoint blockade therapies for two telomere transcriptional gene signatures.

metastatic melanoma harboring the $NRAS^{Q61R}$-positive mutation from a patient who first progressed on pembrolizumab and subsequently on the combination of ipilimumab plus nivolumab. Third, we established PDXs from two $NRAS^{Q61R}$-positive brain metastases derived from a patient with metastatic melanoma and subsequently established two PDXs-derived cell lines, WM4265-1 and WM4265-2. This patient progressed on sequential therapies, including cisplatin, vinblastine, temozolomide, IL2, IFNα-2b, ipilimumab, and pembrolizumab. In addition to therapy-resistant human melanoma, we had access to two derivatives of the mouse melanoma cell line B16: (i) 499 cell line was derived from B16 mouse melanoma that was resistant to radiotherapy and anti-CTLA-4; and (ii) JB2 cell line that differs from 499 in which *PD-L1* was knocked out (28). Finally, we extended our work to nonmelanoma mouse cancer cells that acquired resistance to immune checkpoint blockade therapy to evaluate the efficacy of 6-thio-dG more broadly. This mouse pancreatic cancer cell line G43 was established from mouse pancreatic tumors harboring mutations in *KRAS* and *P53* that progressed on radiotherapy and subsequently ipilimumab.

We treated 13-456-3-3, 13-456-5-3, WM4265-1, WM4265-2, 499, JB2, and G43 cells with 6-thio-dG and observed that prolonged treatment with 6-thio-dG for 12 days markedly inhibited *in vitro* cell proliferation (Fig. 6A). Furthermore, we showed impressive antitumor activity of 6-thio-dG in six xenografts, including 13-456-3-3 (Fig. 6B), 13-456-5-3 (Fig. 6C), 15-1761-1-2 (Fig. 6D), WM4265-2 (Fig. 6E), 499 (Fig. 6F), and G43 (Fig. 6G) when administered intraperitoneally daily.

Using 13-456-5-3 cells and xenografts as a representative pair that was treated with 6-thio-dG *in vitro* and *in vivo*, respectively, we conducted the RPPA experiment and identified proteins that were significantly downregulated by 6-thio-dG. The analysis identified 9 proteins that were commonly downregulated, including phospho-$Myosin^{S1943}$, ARID1A, BRD4, AXL, ATM, eIF4G, PLK1, SOX2, and 53BP1 (Fig. 6H and I). We further extended the RPPA analysis to 5 therapy-resistant cell lines that were treated with 6-thio-dG *in vitro*, including 13-456-3-3, 15-1761-1-2, WM4265-1, WM4265-2, and G43. Importantly, AXL was downregulated in all cell lines except G43 that were treated with 6-thio-dG (Supplementary Fig. S5A–S5E).

In summary, we demonstrated that 6-thio-dG significantly impaired the growth, both *in vitro* and *in vivo*, of melanoma cells derived from various models that acquired resistance to immune checkpoint blockade therapies, implying that 6-thio-dG could be used as a viable therapeutic approach for therapy-resistant melanomas.

Discussion

Following the initial phase of therapeutic responses, patients with unresectable or metastatic melanomas frequently relapse on MAPKi targeting the $BRAF^{V600}$mutations. Molecular mechanisms of acquired resistance to MAPKi are heterogeneous and complex, necessitating the genetic dissection of the mutational spectrum of therapy-resistant tumors to personalize second-line therapies for each individual patient.

Although immune checkpoint blockade therapies that target CTLA4, PD-1, or PD-L1 can elicit durable responses, the majority of patients do not experience durable clinical benefit. For instance, a phase Ib clinical trial demonstrated that the objective response rate was 33% and 45%, respectively, for all patients and treatment-naïve patients treated with pembrolizumab (29). Current studies demonstrate that the lack of response to immune checkpoint blockade therapies is, at least in part, due to expression of the PD-1/PD-L1 immune inhibitory axis, activation of alternative immune checkpoints such as TIM-3, and activation of a melanoma-intrinsic WNT/β-catenin signaling axis, resulting in T-cell exclusion and resistance (30–32).

Because *TERT* promoter mutations are highly prevalent in melanomas resulting in high telomerase activity and molecular mechanisms underlying therapy resistance are heterogeneous, we hypothesized that targeting telomerase activity in therapy-resistant and telomerase-positive tumors might provide a universal strategy to achieve long-term and stable melanoma control.

To therapeutically target telomerase-positive melanomas, we exploited a novel telomere-directed, telomerase-dependent anticancer inhibitor, 6-thio-dG, in a panel of *BRAF*-mutated human melanoma cell lines. Telomerase recognizes the nucleoside 6-thio-dG, which is subsequently incorporated into *de novo*–synthesized telomeres, leading to DNA damage localized at telomeric DNA regions and the rapid killing of cancer cells. Previously, we demonstrated that 6-thio-dG did not lead to weight loss or changes in hematologic, renal, or liver function at effective *in vivo* doses, which was further confirmed by this study (18). Similar to other signaling inhibitors such as the BRAFi, responses of *BRAF*-mutant melanoma cell lines to 6-thio-dG are heterogeneous, although the vast majority was sensitive.

We compared the *in vitro* efficacy of 6-thio-dG to that of PLX4720 and demonstrated 6-thio-dG alone is able to elicit apoptosis and cell death in *BRAF*-mutated melanoma cell lines, including ones that are intrinsically resistant to PLX4720. Extended treatment with 6-thio-dG impairs cell viability and induces cellular senescence in the small fraction of surviving cell, resulting in progressively shortened telomeres, mimicking a phenotype of replicative senescence exhibited by normal cells. We also compared the *in vivo* efficacy of 6-thio-dG to that of another BRAF inhibitor, dabrafenib, and demonstrated that both of them had very similar effect in inhibiting the tumor growth.

To investigate alterations in signaling transduction proteins that are induced by 6-thio-dG, we conducted integrated computational analyses of melanoma cells treated with 6-thio-dG using RNA-seq and RPPA platforms. We discovered that cell cycle, telomere signaling, DNA damage response and molecules causing therapy resistance are decreased in cells treated with 6-thio-dG.

We speculate that short-term treatment with MAPKi might select a subpopulation of *BRAF*-mutated melanoma cells in which AXL and other resistant markers are upregulated and telomere transcriptional gene signatures are enriched, allowing them to adapt to, and evade MAPKi. The "one-two punch" ability of 6-thio-dG to downregulate resistant markers such as AXL among others at the protein level, and induce telomere dysfunction makes it an attractive approach with the potential to overcome both intrinsic and acquired drug resistance to MAPKi. In this study, we demonstrated that 6-thio-dG is able to inhibit the growth of melanoma cells that acquired drug resistance to MAPKi both *in vitro* and *in vivo*. This warrants a future study in which we explore the efficacy of combining MAPKi with 6-thio-dG in overcoming both intrinsic and acquired resistance to MAPKi.

Only a subset of patients with advanced and metastatic melanomas experience long-term and durable clinical benefits from immune checkpoint blockade therapies. To enhance benefit from immune checkpoint blockade, it is critical to dissect and

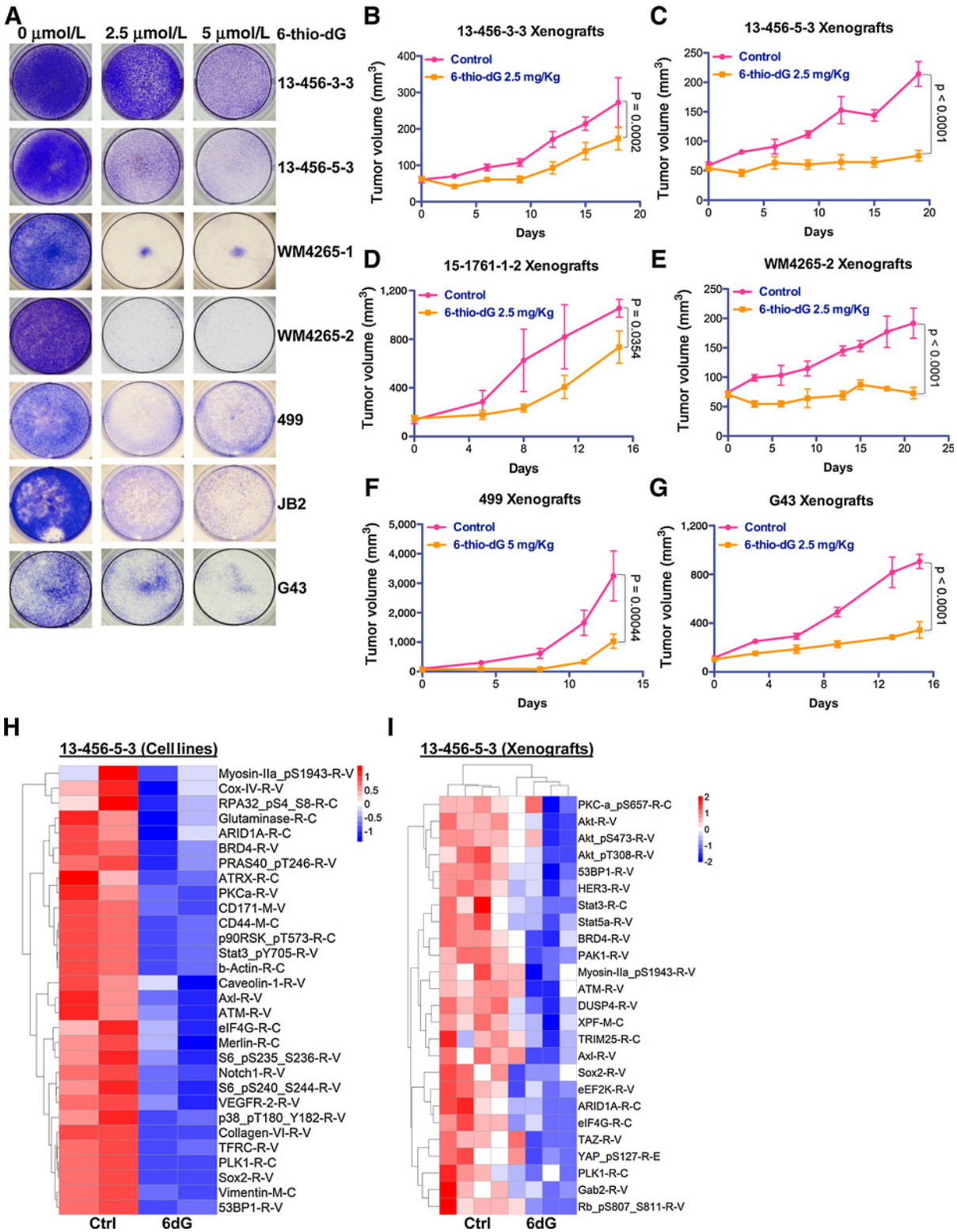

Figure 6.

6-thio-dG impairs cell viability and tumor growth of melanoma cells that are resistant to immune checkpoint blockade therapies when adminstered intraperitoneally daily. **A,** Long-term cell growth assay of 7 patient- or mouse-derived cultures that were treated with 6-thio-dG at indicated doses for 12 days. Cells were then fixed and stained with crystal violet. A representative image of two biological replicates is shown for each experimental sample. **B–G,** Tumor volumes of xenografts of 6 patient- or mouse-derived cultures treated with the vehicle control or 6-thio-dG. **H** and **I,** The heatmap of RPPA data depicting 30 proteins that were most significantly downregulated in 13-456-5-3 cells (**H**) and xenografts (**I**) that were treated with 6-thio-dG (6dG).

therapeutically target molecular mechanisms that underlie adaptive and acquired resistance to immune checkpoint blockade therapies. By analyzing unpaired pre- and posttreatment tumor biopsy specimens derived from patients who did not benefit from ipilimumab as well as paired pre-, on-, and posttreatment tumor biopsy specimens derived from patients who did not benefit from immune checkpoint blockade therapies, we identified "telomeres, telomerase, cellular aging, immortality," "telomere maintenance" and "packaging of telomere ends," that are enriched in on- and/or posttreatment tumor biopsies. Collectively, our data support the notion that the reactivation of the telomere signaling axis could confer a survival advantage upon tumors that are refractory to immune checkpoint blockade therapies.

Having shown that 6-thio-dG is able to prolong the disease control in multiple preclinical models of melanoma cells that acquired resistance to MAPKi, we then hypothesized that 6-thio-dG might also be able to prolong disease control in preclinical models of melanoma cells that acquired resistance to immune checkpoint blockade therapies. Importantly, we demonstrated activity of 6-thio-dG in impairing the growth of short-term primary cultures *in vitro* and *in vivo* that are established from metastatic lesions derived from patients who progress on multiple therapies including ipilimumab and pembrolizumab.

In summary, our current results are highly supportive of using 6-thio-dG as monotherapy following first-line or second-line therapies to prolong disease control of human therapy–resistant and telomerase-positive tumors. This study also paves the way for exploring the combination of 6-thio-dG and first-line therapies in overcoming both intrinsic and acquired resistance.

Disclosure of Potential Conflicts of Interest

L.N. Kwong reports receiving a commercial research grant from Array Biopharma. G.B. Mills reports receiving a commercial research grant from Adelson Medical Research Foundation, AstraZeneca, Critical Outcome Technologies, Komen Research Foundation, NanoString, Breast Cancer Research Foundation, Karus, Illumina, Takeda/Millenium Pharamceuticals, Pfizer, has received speakers bureau honoraria from Symphogen, MedImmune, AstraZeneca, ISIS Pharmaceuticals, Lily, Novartis, ImmunoMet, Allostery, Tarveda, Pfizer, has ownership interest (including patents) Catena Pharmaceuticals, PTV Ventures, Spindletop Ventures, Myriad Genetics, ImmunoMet, and is a consultant/advisory board member for Adventist Health, AstraZeneca, Provista Diagnostics, Signalchem Lifesciences, Symphogen, Lilly, Novartis, Tarveda, Tau Therapeutics, Allostery, Catena Pharmaceuticals, Critical Outcome Technologies, ISIS Pharmaceuticals, ImmunoMet, Takeda/Millenium Pharmaceuticals, MedImmune, and Precision Medicine. J.W. Shay has ownership interest (including patents) in Barricade Therapeutics. No potential conflicts of interest were disclosed by the other authors.

Authors' Contributions

Conception and design: G. Zhang, X. Xu, G.B. Mills, J.W. Shay, M. Herlyn
Development of methodology: G. Zhang, O. Ope, J. Tan, X. Xu, J.W. Shay
Acquisition of data (provided animals, acquired and managed patients, provided facilities, etc.): G. Zhang, L.W. Wu, I. Mender, M. Barzily-Rokni, M.R. Hammond, O. Ope, N. Sadek, M. Xiao, U. Saeed, E. Sugarman, C. Krepler, P.A. Brafford, K. Sproesser, S. Murugan, R. Somasundaram, J. Woo, D.T. Frederick, W. Xu, G.C. Karakousis, X. Xu, L.M. Schuchter, T.C. Mitchell, L.N. Kwong, G. Boland, K.L. Nathanson, G.B. Mills, K.T. Flaherty, T. Vasilopoulos
Analysis and interpretation of data (e.g., statistical analysis, biostatistics, computational analysis): G. Zhang, L.W. Wu, I. Mender, O. Ope, C. Cheng, S. Randell, T. Tian, U. Saeed, E. Sugarman, C. Krepler, R. Somasundaram, B. Wubbenhorst, J. Woo, X. Yin, Q. Liu, R.K. Amaravadi, G. Boland, Z. Wei, K.L. Nathanson, G.B. Mills, K.T. Flaherty, J.W. Shay, M. Herlyn
Writing, review, and/or revision of the manuscript: G. Zhang, L.W. Wu, O. Ope, S. Randell, N. Sadek, U. Saeed, E. Sugarman, Q. Liu, W. Xu, G.C. Karakousis, X. Xu, T.C. Mitchell, R.K. Amaravadi, Z. Wei, K.L. Nathanson, K.T. Flaherty, J.W. Shay, M. Herlyn
Administrative, technical, or material support (i.e., reporting or organizing data, constructing databases): G. Zhang, L.W. Wu, A. Beroard, U. Saeed, J. Woo, B. Miao, W. Xu, R.K. Amaravadi, K.L. Nathanson, T. Vasilopoulos, U. Herbig
Study supervision: G. Zhang, Z. Wei, J.W. Shay
Other (conducted experiments): B. Garman
Other (performed RPPA assay and provided raw data): Y. Lu

Acknowledgments

The research was funded by NIH grants P01CA114046, P50CA174523, P50CA70907, 1U54CA224070, DoD PRCRP grant CA150619, AG01228, the Southland Financial Corporation Distinguished Chair in Geriatric Research, the Dr. Miriam and Sheldon G. Adelson Medical Research Foundation, and the Melanoma Research Foundation; NIH grant 5R01CA136533 to U. Herbig; and by the Tara Miller Foundation to L.M. Schuchter. The support for Shared Resources utilized in this study was provided by Cancer Center Support Grant (CCSG) CA010815 to The Wistar Institute, CA016672 to the MDACC, and CA142543 to UTSW. Part of this work was performed in laboratories constructed with support from NIH grant C06 RR30414. The authors thank all former and current lab members for comments and helpful discussions; J. Hayden and F. Keeney (Wistar Microscopy Facility), C. Chang, S. Billouin, and T. Nguyen (Wistar Genomics Facility), J.S. Faust (Wistar Flow Cytometry Facility), D. DiFrancesco (Wistar Animal Facility), and F. Chen (Wistar Histotechnology Facility) for technical support; and M.B. Powell for providing human melanoma cells (Stanford University). The authors apologize to those whose work was not cited or mentioned here due to space constraints.

The costs of publication of this article were defrayed in part by the payment of page charges. This article must therefore be hereby marked *advertisement* in accordance with 18 U.S.C. Section 1734 solely to indicate this fact.

Received September 22, 2017; revised February 10, 2018; accepted March 15, 2018; published first March 21, 2018.

References

1. Hanahan D, Weinberg RA. Hallmarks of cancer: the next generation. Cell 2011;144:646–74.
2. Huang WF, Hodis E, Xu MJ, Kryukov GV, Chin L, Garraway LA. Highly recurrent TERT promoter mutations in human melanoma. Science 2013; 339:957–9.
3. Horn S, Figl A, Rachakonda PS, Fischer C, Sucker A, Gast A, et al. TERT promoter mutations in familial and sporadic melanoma. Science 2013; 339:959–61.
4. Vinagre J, Almeida A, Pópulo H, Batista R, Lyra J, Pinto V, et al. Frequency of TERT promoter mutations in human cancers. Nat Commun 2013;4:2185.
5. Killela JP, Reitman ZJ, Jiao Y, Bettegowda C, Agrawal N, Diaz LA Jr, et al. TERT promoter mutations occur frequently in gliomas and a subset of tumors derived from cells with low rates of self-renewal. Proc Natl Acad Sci U S A 2013;110:6021–6.
6. Ceccarelli M, Barthel FP, Malta TM, Sabedot TS, Salama SR, Murray BA, et al. Molecular profiling reveals biologically discrete subsets and pathways of progression in diffuse glioma. Cell 2016;164:550–63.
7. Borah S, Xi L, Zaug AJ, Powell NM, Dancik GM, Cohen SB, et al. Cancer. TERT promoter mutations and telomerase reactivation in urothelial cancer. Science 2015;347:1006–10.
8. Weinhold N, Jacobsen A, Schultz N, Sander C, Lee W. Genome-wide analysis of noncoding regulatory mutations in cancer. Nat Genet 2014; 46:1160–5.
9. The Cancer Genome Atlas Network. Genomic classification of cutaneous melanoma. Cell 2015;161:1681–96.
10. Shain AH, Yeh I, Kovalyshyn I, Sriharan A, Talevich E, Gagnon A, et al. The genetic evolution of melanoma from precursor lesions. N Engl J Med 2015;373:1926–36.

11. Heidenreich B, Nagore E, Rachakonda PS, Garcia-Casado Z, Requena C, Traves V, et al. Telomerase reverse transcriptase promoter mutations in primary cutaneous melanoma. Nat Commun 2014;5:3401.
12. Li Y, Zhou QL, Sun W, Chandrasekharan P, Cheng HS, Ying Z, et al. Non-canonical NF-kappaB signalling and ETS1/2 cooperatively drive C250T mutant TERT promoter activation. Nat Cell Biol 2015;17: 1327–38.
13. Bell JR, Rube HT, Kreig A, Mancini A, Fouse SD, Nagarajan RP, et al. Cancer. The transcription factor GABP selectively binds and activates the mutant TERT promoter in cancer. Science 2015;348:1036–9.
14. Johnson BD, Menzies AM, Zimmer L, Eroglu Z, Ye F, Zhao S, et al. Acquired BRAF inhibitor resistance: a multicenter meta-analysis of the spectrum and frequencies, clinical behaviour, and phenotypic associations of resistance mechanisms. Eur J Cancer 2015;51: 2792–9.
15. Rizos H, Menzies AM, Pupo GM, Carlino MS, Fung C, Hyman J, et al. BRAF inhibitor resistance mechanisms in metastatic melanoma: spectrum and clinical impact. Clin Cancer Res 2014;20:1965–77.
16. Roesch A, Paschen A, Landsberg J, Helfrich I, Becker JC, Schadendorf D. Phenotypic tumour cell plasticity as a resistance mechanism and therapeutic target in melanoma. Eur J Cancer 2016;59:109–12.
17. Larkin J, Hodi FS, Wolchok JD. Combined nivolumab and ipilimumab or monotherapy in untreated melanoma. N Engl J Med 2015;373:23–34.
18. Mender I, Gryaznov S, Dikmen ZG, Wright WE, Shay JW. Induction of telomere dysfunction mediated by the telomerase substrate precursor 6-thio-2'-deoxyguanosine. Cancer Discov 2015;5:82–95.
19. Zhang G, Frederick DT, Wu L, Wei Z, Krepler C, Srinivasan S, et al. Targeting mitochondrial biogenesis to overcome drug resistance to MAPK inhibitors. J Clin Invest. 2016;126:1834–56.
20. Lu H, Liu S, Zhang G, Bin Wu, Zhu Y, Frederick DT, et al. PAK signalling drives acquired drug resistance to MAPK inhibitors in BRAF-mutant melanomas. Nature 2017;550:133–6.
21. Dikmen GZ, Gellert GC, Jackson S, Gryaznov S, Tressler R, Dogan P, et al. In vivo inhibition of lung cancer by GRN163L: a novel human telomerase inhibitor. Cancer Res 2005;65:7866–73.
22. Ludlow TA, Robin JD, Sayed M, Litterst CM, Shelton DN, Shay JW, et al. Quantitative telomerase enzyme activity determination using droplet digital PCR with single cell resolution. Nucleic Acids Res 2014;42:e104.
23. Damm K, Hemmann U, Garin-Chesa P, Hauel N, Kauffmann I, Priepke H, et al. A highly selective telomerase inhibitor limiting human cancer cell proliferation. EMBO J 2001;20:6958–68.
24. Patel PL, Suram A, Mirani N, Bischof O, Herbig U. Derepression of hTERT gene expression promotes escape from oncogene-induced cellular senescence. Proc Nat Acad Sci U S A 2016;113:E5024–33.
25. Konieczkowski JD, Johannessen CM, Abudayyeh O, Kim JW, Cooper ZA, Piris A, et al. A melanoma cell state distinction influences sensitivity to MAPK pathway inhibitors. Cancer Discov 2014;4:816–27.
26. Snyder A, Makarov V, Merghoub T, Yuan J, Zaretsky JM, Desrichard A, et al. Genetic basis for clinical response to CTLA-4 blockade in melanoma. N Engl J Med 2014;371:2189–99.
27. Chiappinelli BK, Strissel PL, Desrichard A, Li H, Henke C, Akman B, et al. Inhibiting DNA methylation causes an interferon response in cancer via dsRNA including endogenous retroviruses. Cell 2016;164: 1073.
28. Benci LJ, Xu B, Qiu Y, Wu TJ, Dada H, Twyman-Saint Victor C, et al. Tumor interferon signaling regulates a multigenic resistance program to immune checkpoint blockade. Cell 167:1540–54.e12.
29. Ribas A, Hamid O, Daud A, Hodi FS, Wolchok JD, Kefford R, et al. Association of pembrolizumab with tumor response and survival among patients with advanced melanoma. JAMA 2016;315: 1600–9.
30. Tumeh CP, Harview CL, Yearley JH, Shintaku IP, Taylor EJM, Robert L, et al. PD-1 blockade induces responses by inhibiting adaptive immune resistance. Nature 2014;515:568–71.
31. Spranger S, Bao R, Gajewski TF. Melanoma-intrinsic beta-catenin signalling prevents anti-tumour immunity. Nature 2015;523:231–5.
32. Koyama S, Akbay EA, Li YY, Herter-Sprie GS, Buczkowski KA, Richards WG, et al. Adaptive resistance to therapeutic PD-1 blockade is associated with upregulation of alternative immune checkpoints. Nat Commun 2016;7: 10501.